Organic & Biomolecular Chemistry

PAPER

Synthesis, Properties, and Crystal Structures of π-Extended Double [6]Helicenes: Contorted Multi-Dimensional Stacking Lattice

Received 00th April 20xx,
Accepted 00th April 20xx

DOI: 10.1039/x0xx00000x

www.rsc.org/

Takao Fujikawa,[a] Nobuhiko Mitoma,[a,b] Atsushi Wakamiya,[c] Akinori Saeki,[d] Yasutomo Segawa,*[,a,b] and Kenichiro Itami*[,a,b,e,f]

The synthesis and properties of a new π-extended double [6]helicene **2** and a dithia[6]helicene **3** are described. Compared to the previously reported parent double-helicene molecule **1**, the introduction of *n*-butyl groups successfully improved the solubility, which allowed an experimental investigation into the electronic structure of **2** and **3** by photophysical measurements and cyclic voltammetry. The characteristic two-blade propeller structures of **2** and **3** were unambiguously determined by single-crystal X-ray diffraction analysis. The crystal packing structure of **2** exhibited a contorted two-dimensional stacking, whereby molecules of *n*-pentane were incorporated in the stacks. Despite the presence of *n*-butyl groups, **3** formed a unique three-dimensional stacking lattice in the crystal. Time-resolved microwave conductivity measurements revealed that the double helicenes (**1–3**) exhibited transient conductivities. An organic field-effect transistor fabricated using **3** was found to function as a p-type transistor.

Introduction

Over the past few decades, chemists have made enormous efforts to achieve control over the molecular packing of π-conjugated molecules in order to exploit the outstanding electronic and/or optical properties of these compounds.[1] A central theme of these efforts is the introduction of substituents such as long alkyl chains,[2] bulky substituents,[3] and noncovalent bonding entities[4] onto the periphery of the planar π-systems (Figure 1A). Even though this strategy has been quite effective for the design of one- and two-dimensional stacking modes (e.g., herringbone and lamellar types), it is unfortunately unsuitable for the design of three-dimensional stacking modes.

Another principal theme is based on employing intrinsically curved π-systems, as a disruption of the planarity of the π-system can diversify the molecular filling (Figure 1B).[1f,g,i,j,m] In this respect, the most prominent example is fullerenes, whose spherical π-systems can provide omnidirectional π–π interactions, which render these compounds essential isotropic materials in the context of organic electronics.[5] Apart from fullerenes, multihelicenes have emerged in recent years as another fascinating class of nonplanar π-systems.[6,7] In some cases, their propeller-shaped π-systems, comprising several π-blades, can facilitate unconventional multi-dimensional π–π

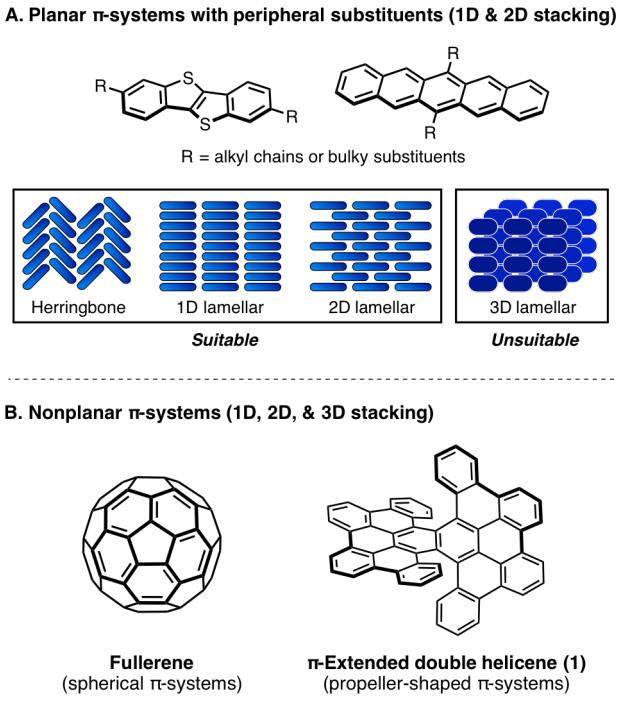

Fig. 1 Two principle strategies to control the molecular packing of π-conjugated molecules: (A) introduction of peripheral substituents, and (B) intrinsically curved π-systems.

[a] *Graduate School of Science, Nagoya University, Chikusa, Nagoya 464-8602, Japan. E-mail: ysegawa@nagoya-u.jp (Y.S.), itami@chem.nagoya-u.ac.jp (K.I.)*
[b] *JST, ERATO, Itami Molecular Nanocarbon Project, Nagoya University, Japan.*
[c] *Institute for Chemical Research, Kyoto University, Uji, Kyoto 611-0011, Japan.*
[d] *Department of Applied Chemistry, Graduate School of Engineering, Osaka University, 2-1 Yamadaoka, Suita, Osaka, 565-0871, Japan.*
[e] *Institute of Transformative Bio-Molecules (WPI-ITbM), Nagoya University, Japan.*
[f] *Integrated Research Consortium on Chemical Science, Nagoya University, Japan.*
Electronic Supplementary Information (ESI) available: Detailed experimental procedures, computational studies, and spectral data for all compounds. CCDC 1542924 (**2**), 1542925 (**3**). See DOI: 10.1039/x0xx00000x

stacking with cofacial π–π overlap.[7a,b,f] One such example is the π-extended double [6]helicene (**1**), which we have recently reported.[7e] As a consequence of the two relatively planar π-blades connected in a twisted fashion, a contorted three-dimensional lamellar packing was observed for **1** in the crystalline state.

Herein, we describe the continuation of our investigations regarding the chemistry of π-extended double helicenes. With a view toward applications in semiconducting materials, new double [6]helicenes were designed with the support of theoretical calculations in order to improve their solubility and to modulate their frontier molecular orbitals (FMOs). A modular synthesis of the thus-designed compounds **2** and **3** was accomplished by the Scholl reaction of tetrasubstituted naphthalene derivatives, and their fundamental electronic properties were examined. As expected from the molecular packing of **1**, fascinating multi-dimensional stacking structures were observed for **2** and **3**. When **3** was incorporated in an organic field-effect transistor, its unique three-dimensional π–π stacking lattice resulted in p-type semiconducting properties with a hole mobility of 3.3×10^{-2} $cm^2 \cdot V^{-1} \cdot s^{-1}$.

Results and discussion

Molecular design

The parent π-extended double [6]helicene **1** consists exclusively of hydrogen and sp^2-hybridized carbon atoms. Therein, two relatively planar tribenzo[*b,n,pqr*]perylene moieties (π-blades) are concatenated to afford the characteristic two-blade propeller structure. The thus-formed fully-conjugated [6]helicene substructures afford enantiomers of *twisted*-isomers, i.e., (*P,P*)-**1** and (*M,M*)-**1**. In the crystalline state, these enantiomers arrange in offset three-dimensional stacks. While this unique racemic crystal structure stimulated our interest in the application of **1** as a semiconducting material, its prohibitively low solubility in common organic solvents has so far hampered device fabrication. Another shortcoming of **1** is the pronounced naphthalene-like distribution of the FMOs at the center of the molecule due to the heavily twisted π-conjugation. The molecular orbitals of **1** in the crystalline state overlap intermolecularly via the periphery of the π-system. Therefore, in order to gain larger transfer integrals, the molecular design should afford molecules that contain FMOs with a large distribution on the periphery of the two π-blades.

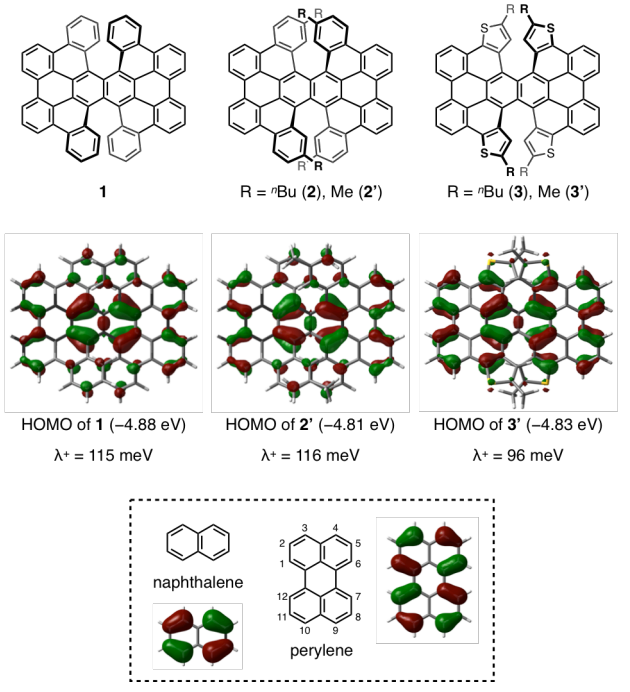

Fig. 2 Structures of **1–3**, naphthalene, and perylene, together with estimated distributions (isovalue = 0.03) and energy levels of the HOMOs; DFT calculations at the B3LYP/6-31G(d) level of theory were conducted.

To satisfy the aforementioned requirements, we designed new π-extended double [6]helicenes **2** and **3** (Figure 2). In both cases, four *n*-butyl groups were introduced at the terminal aromatic rings of the helical moieties in order to improve the solubility. Density functional theory (DFT) calculations at the B3LYP/6-31G(d) level of theory were performed for **1**, **2'**, and **3'**, where **2'** and **3'** represent the methyl analogues of **2** and **3**, respectively. When comparing **1** with **2'**, negligible influence of these alkyl groups was predicted on the distributions and the energy levels of the HOMOs (**1**: −4.88 eV; **2'**: −4.81 eV), and the reorganization energies (λ) of hole transfer (**1**: λ^+ = 115 meV; **2'**: λ^+ = 116 meV). In contrast, the FMOs of **3'**, which exhibits a dithia[6]helicene moiety instead of all-carbon [6]helicene substructures, displayed an enhanced distribution on the periphery of π-system. This is presumably due to the lower aromaticity of the thiophene rings relative to that of benzene rings, resulting in a perylene-like distribution of the FMOs on the two π-blades. Such delocalization of the HOMO effectively lowered the reorganization energy (**3'**: λ^+ = 96 meV). In addition, we anticipated improved semiconducting properties for **3**, considering that several thiophene-containing π-conjugated molecules are excellent hole-transporting materials.[8]

Synthesis and configurations

The synthetic routes to **2** and **3** are shown in Scheme 1. Previously, **1** was synthesized from naphthalene derivative **4** via the introduction of four biphenyl units under Suzuki–Miyaura cross-coupling conditions, followed by oxidative stitching using the Scholl reaction. Target compounds **2** and **3** were prepared according to a similar modular synthesis starting from **4**.

For the synthesis of **2**, **6** was prepared by a fourfold Suzuki–Miyaura coupling reaction of **5** with **4**. The subsequent oxidative stitching in the presence of $MoCl_5$ afforded the *twisted*-isomers of **2**, i.e., (*P,P*)-**2** and (*M,M*)-**2**, in 13% yield.[9] In contrast to the synthesis of **1**, the *meso*-isomer of **2**, i.e., (*P,M*)-**2**, was not detected. We suspect that the *meso*-isomer of **2** is intolerant of the applied oxidative reaction conditions due to the improved solubility, and that the *twisted*-isomers were therefore obtained exclusively.

The synthesis of **3** was accomplished by the Scholl reaction of the naphthalene derivative **7** that has also been used recently for the synthesis of quadruple helicenes.[7d] We have previously reported that the treatment of **7** with $MoCl_5$ (10 equiv) in the presence of molecular sieves results in a fourfold C–C bond formation. In the present study, we found that using a slight excess of $MoCl_5$ (20 equiv)[10] generates tetrachlorinated **8** in 26% yield, while lowering the proportion of the oxidant (12, 14, or 16 equiv) did not afford well-defined products. It is likely that the chlorination took place immediately after cyclization, and the introduced chlorine atoms served to cap the reactive sites of intermediate **3**, corresponding to the most nucleophilic positions of perylene (3, 4, 9, and 10), for unfavorable side reactions such as polymerization and decomposition.[11] This assumption is consistent with the enhanced perylene-like distribution of the HOMO of **3**.[12] Thus, chlorination, which is often avoided during oxidative stitching, plays an important role in the synthesis of **8**. Finally, a subsequent palladium-catalyzed dechlorination of **8** quantitatively furnished the target double helicene **3**.[13] A single-crystal X-ray diffraction analysis of **3** (*vide infra*) revealed that the configuration of the obtained double helicene is commensurate with the *twisted*-isomers (*P,P*)-**3** and (*M,M*)-**3**. Similar to the synthesis of **2**, the *meso*-isomers (*P,M*)-**3** or (*P,M*)-**8** were not detected.

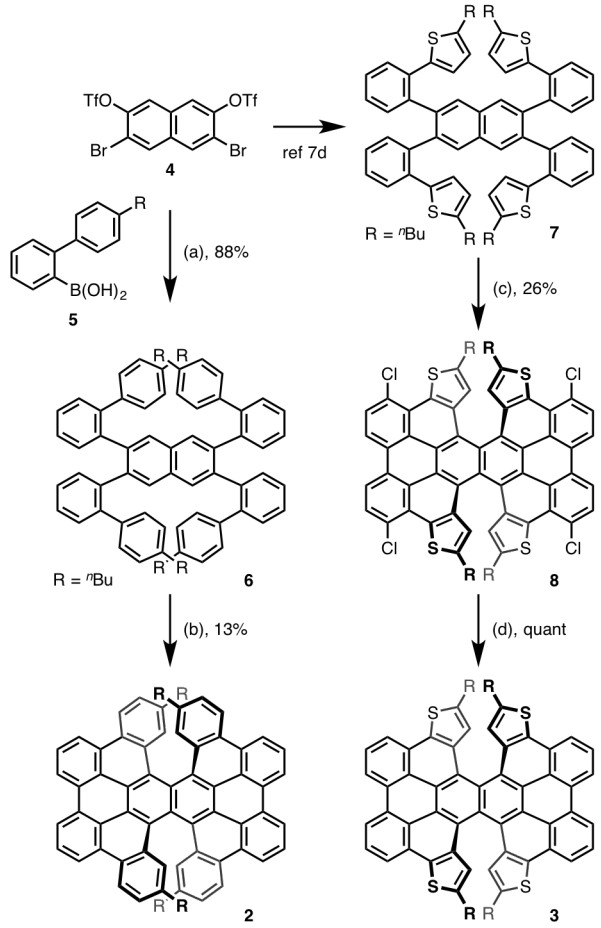

Scheme 1 Synthesis of π-extended double [6]helicenes. Reaction conditions: (a) **5** (ca. 8 equiv), $Pd(OAc)_2$ (5 mol%), SPhos (10 mol%), K_3PO_4 (8 equiv), toluene, 100 °C, 72 h; (b) $MoCl_5$ (15 equiv), CH_2Cl_2 (5 mM), 0 °C to RT, 72 h; (c) $MoCl_5$ (20 equiv), CH_2Cl_2 (5 mM), RT, 40 min; (d) Pd/C, HCO_2H, Et_3N, pyridine, 130 °C, 25 h.

To elucidate the thermodynamic stability and the dynamic behavior of the diastereomers of **3**, DFT calculations were carried out at the B3LYP/6-31G(d) level for the *twisted*-isomers, the *meso*-isomers, and the interjacent transition states. Previously, we have already predicted that *twisted*-**1** should be thermodynamically more stable than *meso*-**1** (0.9 kcal·mol^{-1}) and that the activation barrier for the *twisted*-to-*meso* interconversion should amount to 43.5 kcal·mol^{-1} (Figure 3a and Figure S4a). It should also be noted that in the case of dithia[6]helicene **3'**, *meso*-**3'** is substantially destabilized (7.2 kcal·mol^{-1}) relative to *twisted*-**3'** (Figure 3b and Figure S4b).

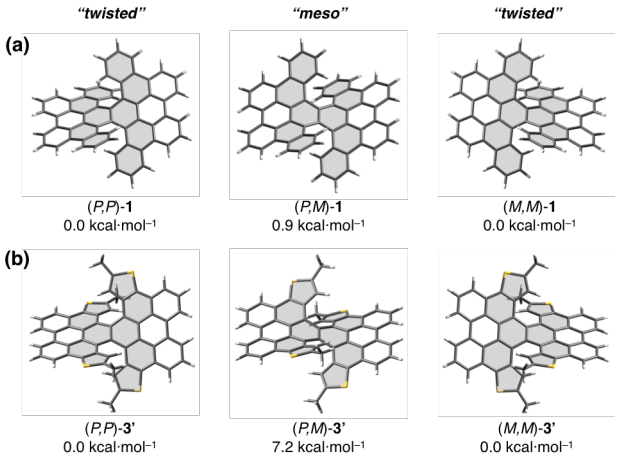

Fig. 3 Diastereomers and relative energies of (a) **1**[7e] and (b) **3'**; for the DFT calculations at the B3LYP/6-31G(d) level of theory, the *n*-butyl groups were replaced with methyl groups.

The absence of *meso*-**8** after the Scholl reaction could thus be attributed to the inaccessibility of *meso*-**3** during the oxidative cyclization, which may be explained by its highly strained structure. A significant destabilization was also observed for the transition state of the *twisted*-to-*meso* interconversion of **3'**, for which an activation barrier of 50.8 kcal·mol^{-1} was estimated. To our knowledge, this estimated barrier is the highest value among the ever-reported double helicenes.[7J,k] We attributed this high barrier to the difference of the direction of the internal C–H bonds within the helixes. On account of the smaller interior bond angles of the thiophene rings, the congestion between the two C–H bonds within the helix should prevent the two helical termini to get into close spatial proximity during the transition state compared to those of carbo[6]helicenes. Indeed, a closer proximity of the hydrogen atoms within the helix was observed in the optimized transition state of **3'** (1.81 Å) relative to that of **1** (1.88 Å), inferring a larger steric demand. In a previous report, we have already confirmed that the isomerization of *meso*-**1** to *twisted*-**1** requires high temperature (> 230 °C). Therefore, although the optical separation of **3** was unsuccessful, its interconversion should need severely elevated temperatures and should thus be difficult to observe.

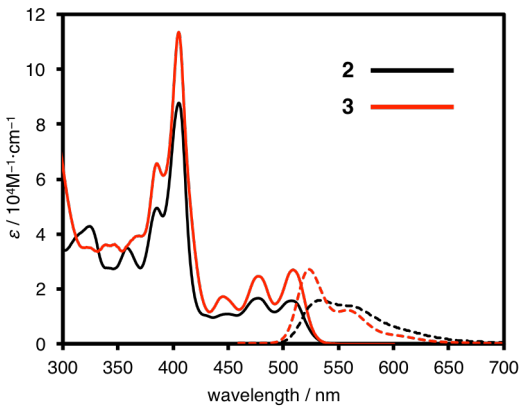

Fig. 4 UV–vis absorption (solid lines) and fluorescence spectra (dashed lines) for **2** (black) and **3** (red) in chloroform.

Photophysical and electrochemical properties

The photophysical properties of **2** and **3** were measured in chloroform (Figure 4). The UV–vis absorption spectrum of **2** was almost identical to that of **1** (Figure S1), exhibiting absorption peaks at 507, 477, and 450 nm, and the most intense peak at 405 nm. Dithia[6]helicene analog **3** afforded a similar absorption spectrum, with a hyperchromic effect and a clearer vibronic structure. Absorption peaks for **3** were observed at 509, 477, 445, and 405 nm, and the peak at 405 nm was most intense. A clear vibronic structure was also observed for the fluorescence spectrum of **3**, which exhibited maxima at 524 and 558 nm. These maxima are comparable, yet slightly blue-shifted relative to those of **2** (534 nm and a shoulder emission at ~560 nm). Notably, the fluorescence quantum yield of **3** (Φ_F = 0.20) was much higher than those of carbohelicene congeners (Φ_F = 0.052 for *twisted*-**1**; 0.059 for *twisted*-**2**), which suggests a distinctive influence of the helical substructures on the entire π-systems.

The improved solubility in organic solvents enabled us to investigate the electrochemical behavior of these π-extended double helicenes in dichloromethane by cyclic voltammetry (Figure 5). Both **2** and **3** exhibited reversible two-step oxidation

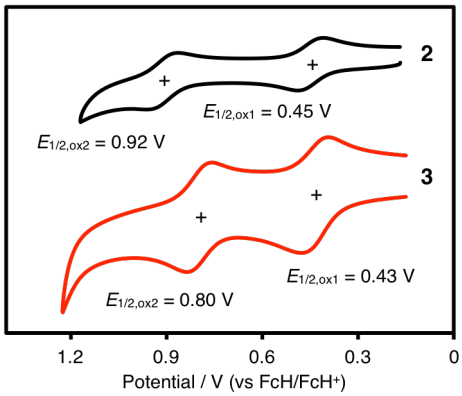

Fig. 5 Cyclic voltammograms of **2** (black) and **3** (red); solvent: dichloromethane; supporting electrolyte: 0.1 M [(*n*-Bu)$_4$N][PF$_6$]; scan rate: 0.1 V·s^{-1}; FcH = ferrocene.

waves with half-wave potentials ($E_{1/2}$) of 0.45 V and 0.92 V for **2**, and 0.43 V and 0.80 V for **3** (vs. FcH/FcH$^+$), indicating good electrochemical stability of the oxidized species. As indicated by the DFT-derived HOMO energy levels, a negligible difference regarding the first oxidation potential was observed between carbo[6]helicene **2** and dithia[6]helicene **3**. In contrast, a moderate cathodic shift of the second oxidation potential (0.12 V) was observed for **3**, which may be rationalized in terms of a stabilization of the cation by the sulfur atoms.

Crystal structures

Single-crystal X-ray diffraction analyses were carried out using racemic single crystals of **2** and **3**. The former were obtained by recrystallization of **2** from chloroform and *n*-pentane, while the latter were obtained by recrystallization of **3** from hot nitrobenzene (Figure 6). Similar to **1**, heavily twisted two-blade propeller structures were observed in both cases. The twisting distortion of **2** and **3** in the crystal was determined using the dihedral angles of the mean planes of the two π-blades (**2**: 52.0°; **3**: 52.1°). These values are slightly larger than the corresponding angle in **1** (47.2°). Theoretically, on the B3LYP/6-31G(d) level of theory, twisting distortions of 46.6° (**1**, **2**) and 50.1° (**3**) were estimated for the optimized structures of **1**, **2'** and **3'**. Considering that the theoretical predictions suggest that a substitution with alkyl groups should hardly affect the molecular geometry, we tentatively assigned the larger distortion of **2** compared to **1** in the crystals to the difference in the molecular packing structures and the associated intermolecular interactions. These profound distortions of the π-system should give rise to unique multi-dimensional stacking structures.

Unlike **1**, a contorted two-dimensional stacking was observed in the crystals of **2**, whereby molecules of *n*-pentane were inserted within the stacks (Figure 6b,c). Three types of π–π stacking can be distinguished: two of them form a slipped one-dimensional heterochiral stacking along the *a*-axis with an interplanar distance ($d_{\pi-\pi}$) of 3.37 Å and 3.40 Å, respectively, while the other connects the aforementioned stacking columns in the direction of the *b*-axis ($d_{\pi-\pi}$ = 3.38 Å). Consequently, a two-dimensional stacking layer spreads over the *ab*-plane, and the *n*-butyl groups fill the gap between neighboring layers, thus preventing an interlayer electronic interaction along the *c*-axis.

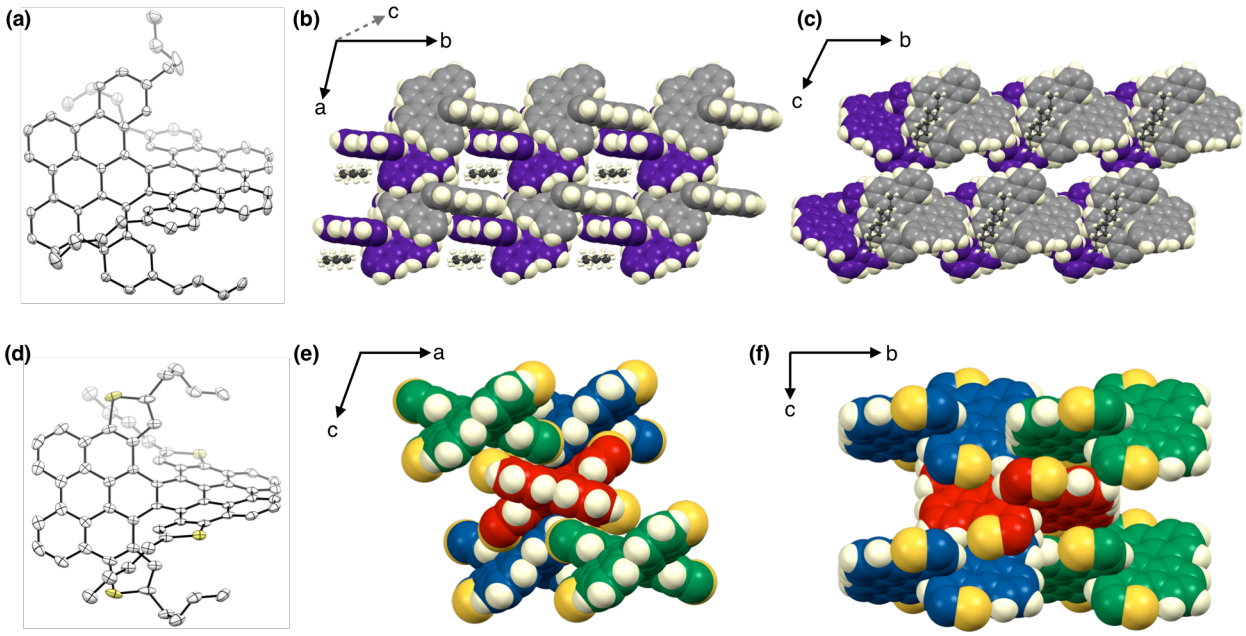

Fig. 6 ORTEP drawings of (a) (*M*,*M*)-**2** and (d) (*M*,*M*)-**3** (atomic displacement parameters set at 50% probability; hydrogen atoms and the minor part of the disordered moieties are omitted for clarity; for **2**, one molecule of *n*-pentane is omitted). (b,c) Packing structure of **2** (*n*-butyl groups are omitted for clarity; π-skeletons and *n*-pentane molecules are depicted using a space-filling model and a ball-and-stick model, respectively; (*P*,*P*)-**2**: purple; (*M*,*M*)-**2**: gray). (e,f) Packing structure of **3** (*n*-butyl groups are omitted for clarity; homochiral molecules on the same *ac*-plane are colored in blue, red, and green).

More intriguingly, the crystal structure of **3** displayed a unique contorted three-dimensional stacking lattice (Figure 6e,f). In these crystals, one of the two π-blades per molecule (red molecule) participates in a slipped one-dimensional heterochiral stacking ($d_{\pi-\pi}$ = 3.43 Å) illustrated by the stacking along the blue–red–blue molecules, while the other π-blade participates in a slipped one-dimensional heterochiral stacking ($d_{\pi-\pi}$ = 3.51 Å) in a different direction, illustrated by the stacking along the green–red–green molecules. These alternately arranged two types of stacking columns are electronically connected to each other through the red molecule, providing an unprecedented three-dimensional lattice of π–π stacking as the whole crystal structure. In this way, it was proved that the planarity of two π-blades facilitates cofacial π-interactions, whereas the nonplanarity as the entire molecule dramatically alters the way of molecular filling.

Conductive behavior

The good reversibility of the electrochemical oxidation and the unique molecular packing in **2** and **3** motivated us to investigate their semiconducting properties. Initially, we carried out time-resolved microwave conductivity (TRMC) measurements[14a] on crushed crystals of **1**–**3**, in order to estimate their charge transport properties (Figure 7a and Figure S2). The highest TRMC signal maximum ($\phi\Sigma\mu_{max}$) was observed for **3** (1.1×10^{-4} $cm^2\cdot V^{-1}\cdot s^{-1}$; ϕ: photo-generation efficiency of the charge carrier; $\Sigma\mu$: local mobility), followed by **1** (7.8×10^{-5} $cm^2\cdot V^{-1}\cdot s^{-1}$) and **2** ($6.1\times10^{-5}$ $cm^2\cdot V^{-1}\cdot s^{-1}$). These values are mostly comparable with those found in a triphenylene derivative with columnar π–π stacking[14b] and a tetracene derivative with CH–π stacking,[14c] which clearly demonstrates the charge transport ability of π-extended double [6]helicenes.

Considering its high TRMC signal, its solubility in organic solvents, the absence of solvent molecules in its crystal structure, and its low reorganization energy, we also examined the semiconducting properties of **3**. For that purpose, a top-contact/bottom-gate transistor was fabricated on Si/SiO_2 substrates by a drop-coat method using toluene solutions of **3**,

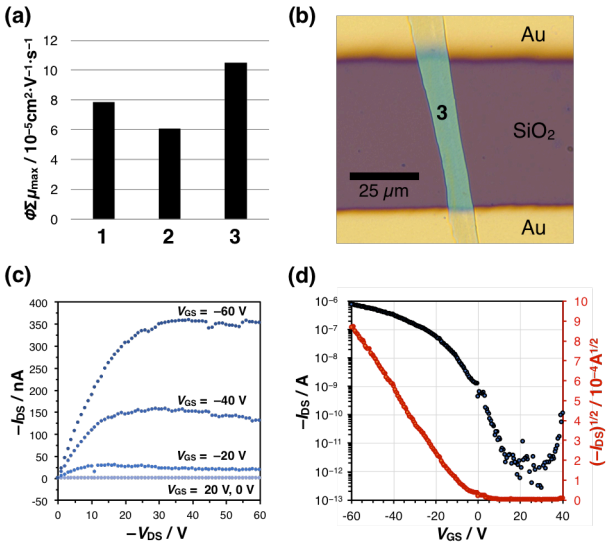

Fig. 7 (a) Results of the TRMC measurements of **1**–**3**. (b) Optical microscope image of the OFET of **3** fabricated on a Si/SiO_2 substrate. (c) Output and (d) transfer characteristics of **3** (V_{DS} = −60 V).

and subsequent gold electrode evaporation (Figure 7b, see the Supporting Information for details). The output and transfer characteristics are shown in Figure 7c,d. The field-effect transistor of the thin film of **3** functioned as a p-type semiconductor, exhibiting a hole mobility (μ_h) of 3.3×10^{-2} $cm^2\cdot V^{-1}\cdot s^{-1}$ in an inert atmosphere with an on/off ratio of greater than 10^5. The conductive behavior observed herein renders the promising prospects of π-extended double [6]helicenes for organic semiconducting materials with unique molecular packing.

Conclusions

In summary, we disclosed the synthesis of new π-extended double [6]helicenes **2** and **3**. A modular synthesis of these compounds via oxidative stitching from naphthalene derivatives demonstrated the synthetic diversity of our method for the preparation of distorted π-systems. A comparison of carbo[6]helicene **2** and dithia[6]helicene **3** showed that an annulation with thiophene rings results in various perturbations on the double helical π-system, including the distribution of FMOs, the reorganization energy of hole transfer, the thermodynamic stability of diastereomers, the interconversion barriers, the photophysical properties, and the electrochemical behavior. Single-crystal X-ray diffraction analyses revealed that the two-blade propeller molecular geometries display multi-dimensional π–π stacking. The crystal structure of **3** is particularly noteworthy, as it showed an unprecedented three-dimensional π–π stacking lattice consisting of two distinct slipped stacking. TRMC measurements confirmed charge transport properties for these π-extended double [6]helicenes, and indeed, an organic field-effect transistor using **3** on a Si/SiO_2 substrate functions as a p-type transistor with a hole mobility of 3.3×10^{-2} $cm^2\cdot V^{-1}\cdot s^{-1}$. The dimensionality of the molecular packing is a critical factor for the fine-tuning of organic molecular materials.[15] Hence, the nonplanar π-systems enabling multi-dimensional stacking lattices would be a new platform for crystal engineering and molecular assembly to explore materials science.

Acknowledgements

This work was supported by the ERATO program from JST (JPMJER1302 to K.I.), the Funding Program for KAKENHI from MEXT (16K05771 to Y.S., JP26288093 to A.W., and JP15K13816 to A.S.). T.F. is a recipient of JSPS fellowship for young scientists. We greatly thank Prof. Kendal N. Houk (University of California, Los Angeles) and Dr. Ilhan Yavuz (Marmara University) for discussion and support. Calculations were performed using the resources of the Research Center for Computational Science, Okazaki, Japan. ITbM is supported by the World Premier International Research Center (WPI) Initiative, Japan.

Notes and references

1 For selected examples on the control over molecular packing for functional materials, see: (a) Y. Yamaguchi, M. Takubo, K. Ogawa, K. Nakayama, T. Koganezawa, H. Katagiri, *J. Am. Chem. Soc.,* 2016, **138**, 11335; (b) A. T. Haedler, K. Kreger, A. Issac, B. Wittmann, M. Kivala, N. Hammer, J. Köhler, H.-W. Schmidt, R. Hildner, *Nature,* 2015, **523**, 196; (c) Y. Yamaguchi, K. Ogawa, K. Nakayama, Y. Ohba, H. Katagiri, *J. Am. Chem. Soc.,* 2013, **135**, 19095; (d) R. Bhola, P. Payamyar, D. J. Murray, B. Kumar, A. J. Teator, M. U. Schmidt, S. M. Hammer, A. Saha, J. Sakamoto, A. D. Schlüter, B.T. King, *J. Am. Chem. Soc.,* 2013, **135**, 14134; (e) P. Kissel, R. Erni, W. B. Schweizer, M.D. Rossell, B.T. King, T. Bauer, S. Götzinger, A. D. Schlüter, J. Sakamoto, *Nat. Chem.,* 2012, **4**, 287; (f) T. Hatakeyama, S. Hashimoto, T. Oba, M. Nakamura, *J. Am. Chem. Soc.,* 2012, **134**, 19600; (g) S. Pola, C.-H. Kuo, W.-T. Peng, M.M. Islam, I. Chao, Y.-T. Tao, *Chem. Mater.,* 2012, **24**, 2566; (h) F. Würthner, T. E. Kaiser, C. R. Saha-Möller, *Angew. Chem., Int. Ed.* 2011, **50**, 3376; (i) T. Amaya, S. Seki, T. Moriuchi, K. Nakamoto, T. Nakata, H. Sakane, A. Saeki, S. Tagawa, T. Hirao, *J. Am. Chem. Soc.,* 2009, **131**, 408; (j) T. E. Kaiser, H. Wang, V. Stepanenko, F. Würthner, *Angew. Chem., Int. Ed.,* 2007, **46**, 5541, (k) S. Bhosale, A. L. Sisson, P. Talukdar, A. Fürstenberg, N. Banerji, E. Vauthey, G. Bollot, J. Mareda, C. Röger, F. Würthner, N. Sakai, S. Matile, *Science,* 2006, **313**, 84; (l) H. Tanaka, Y. Okano, H. Kobayashi, W. Suzuki, A. Kobayashi, *Science,* 2001, **291**, 285; (m) T. Verbiest, S. V. Elshocht, M. Kauranen, L. Hellemans, J. Snauwaert, C. Nuckolls, T. J. Katz, A. Persoons, *Science,* 1998, **282**, 913.

2 J. Mei, Y. Diao, A. L. Appleton, L. Fang, Z. Bao, *J. Am. Chem. Soc.,* 2013, **135**, 6724.

3 (a) L. Zhang, Y. Cao, N. S. Colella, Y. Liang, J.-L. Brédas, K. N. Houk, A. L. Briseno, *Acc. Chem. Res.,* 2015, **48**, 500; (b) L. Zhang, A. Fonari, Y. Zhang, G. Zhao, V. Coropceanu, W. Hu, S. Parkin, J.-L. Brédas, A. L. Briseno, *Chem. Eur. J.,* 2013, **19**, 17907; (c) J. E. Anthony, J. S. Brooks, D. L. Eaton, S. R. Parkin, *J. Am. Chem. Soc.,* 2001, **123**, 9482.

4 (a) M. Gsänger, J. H. Oh, M. Könemann, H. W. Höffken, A.-M. Krause, Z. Bao, F. Würthner, *Angew. Chem., Int. Ed.,* 2010, **49**, 740; (b) J. C. Genereux, J. K. Barton, *Chem. Rev.,* 2010, **110**, 1642; (c) K. Kobayashi, H. Masu, A. Shuto, K. Yamaguchi, *Chem. Mater.,* 2005, **17**, 6666; (d) D. B. Werz, R. Gleiter, F. Rominger, *J. Am. Chem. Soc.,* 2002, **124**, 10638.

5 (a) W. I. F. David, R. M. Ibberson, J. C. Matthewman, K. Prassides, T. J. S. Dennis, J. P. Hare, H. W. Kroto, R. Taylor, D. R. M. Walton, *Nature,* 1991, **353**, 147; (b) A. Hirsch, M. Brettreich, *Fullerenes: Chemistry and Reactions*, Wiley-VCH, Weinheim, 2005. (c) *Fullerenes: Chemistry, Physics, and Technology* (Eds.: K. M. Kadish, R. S. Ruoff), Wiley, New York, 2000. (d) *Fullerenes: Principles and Applications* (Eds.: F. Lang, J.-F. Nierengarten), RSC, Cambridge, 2007.

6 Reviews on helicenes: (a) M. Gingras, *Chem. Soc. Rev.,* 2013, **42**, 968, (b) M. Gingras, G. Félix, R. Peresutti, *Chem. Soc. Rev.,* 2013, **42**, 1007; (c) M. Gingras, *Chem. Soc. Rev.,* 2013, **42**, 1051; (d) Y. Shen, C.-F. Chen, *Chem. Rev.,* 2012, **112**, 1463.

7 For recent examples of multihelicenes, see: (a) D. Meng, H. Fu, C. Xiao, X. Meng, T. Winands, W. Ma, W. Wei, B. Fan, L. Huo, N. L. Doltsinis, Y. Li, Y. Sun, Z. Wang, *J. Am. Chem. Soc.,* 2016, **138**, 10184; (b) T. Katayama, S. Nakatsuka, H. Hirai, N. Yasuda, J. Kumar, T. Kawai, T. Hatakeyama, *J. Am. Chem. Soc.,* 2016, **138**, 5210; (c) X.-Y. Wang, A. Narita, W. Zhang, X. Feng, K. Müllen, *J. Am. Chem. Soc.,* 2016, **138**, 9021. (d) T. Fujikawa, Y. Segawa, K. Itami, *J. Am. Chem. Soc.,* 2016, **138**, 3587; (e) T. Fujikawa, Y. Segawa, K. Itami, *J. Am. Chem. Soc.,* 2015, **137**, 7763; (f) L. Shan, D. Liu, H. Li, X. Xu, B. Shan, J.-B. Xu, Q. Miao, *Adv. Mater.* 2015, **27**, 3418; (g) X. Gu, X. Xu, H. Li, Z. Liu, Q. Miao, *J. Am. Chem. Soc.* 2015, **137**, 16203; (h) H. Kashihara, T.

Asada, K. Kamikawa, *Chem. Eur. J.,* 2015, **21**, 6523; (i) J. Luo, X. Xu, R. Mao, Q. Miao, *J. Am. Chem. Soc.,* 2012, **134**, 13796; (j) Y. Hu, X.-Y. Wang, P.-X. Peng, X.-C. Wang, X.-Y. Cao, X. Feng, K. Müllen, A. Narita, *Angew. Chem. Int. Ed.* **2017**, *56*, 3374; (k) X.-Y. Wang, X.-C. Wang, A. Narita, M. Wagner, X.-Y. Cao, X. Feng, K. Müllen, *J. Am. Chem. Soc.* **2016**, *138*, 12783.

8 K. Takimiya, S. Shinamura, I. Osaka, E. Miyazaki, *Adv. Mater.,* 2011, **23**, 4347.

9 For a review on the Scholl reaction, see: M. Grzybowski, K. Skonieczny, H. Butenschön, D. T. Gryko, *Angew. Chem., Int. Ed.,* 2013, **52**, 9900.

10 (a) B. T. King, J. Kroulík, C. R. Robertson, P. Rempala, C. L. Hilton, J. D. Korinek, L. M. Gortari, *J. Org. Chem.,* 2007, **72**, 2279; (b) S. Kumar, M. Manicham, *Chem. Commun.,* 1997, 1615.

11 (a) P. Kovacic, M. B. Jones, *Chem. Rev.,* 1987, **87**, 357; (b) P. Rempala, J. Kroulík, B. T. King, *J. Org. Chem.,* 2006, **71**, 5067; (c) P. Kovacic, R. M. Lange, *J. Org. Chem.,* 1963, **28**, 968.

12 Perylene dimerizes under oxidative conditions, see: R. Thamatam, S. L. Skraba, R. P. Johnson, *Chem. Commun* 2013, **49**, 9122.

13 (a) A. M. Butterfield, B. Gilomen, J. S. Siegel, *Org. Process Res. Dev.,* 2012, **16**, 664; (b) M. K. Anwer, D. B. Sherman, J. G. Roney, A. F. Spatola, *J. Org. Chem.,* 1989, **54**, 1284.

14 (a) A. Saeki, Y. Koizumi, T. Aida, S. Seki, *Acc. Chem. Res.,* 2012, **45**, 1193; (b) T. Osawa, T. Kajitani, D. Hashizume, H. Ohsumi, S. Sasaki, M. Takata, Y. Koizumi, A. Saeki, S. Seki, T. Fukushima, T. Aida, *Angew. Chem., Int. Ed.,* 2012, **51**, 7990; (c) T. Okamoto, K. Nakahara, A. Saeki, S. Seki, J. H. Oh, H. B. Akkerman, Z. Bao, Y. Matsuo, *Chem. Mater.,* 2011, **23**, 1646.

15 (a) L. A. Stevens, K. P. Goetz, A. Fonari, Y. Shu, R. M. Williamson, J.-L. Brédas, V. Coropceanu, O. D. Jurchescu, G. E. Collis, *Chem. Mater.,* 2015, **27**, 112; (b) I. Yavuz, B. Martin, J. Park, K. N. Houk, *J. Am. Chem. Soc.,* 2015, **137**, 2856.

Organic & Biomolecular Chemistry

PAPER

TOC

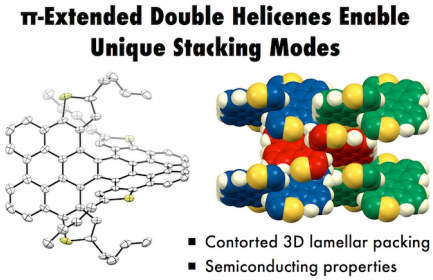

Synthesis, structures, packing modes, and electronic properties of two π-extended double helicene molecules are described.